Simulated Antarctic precipitation and surface mass balance at the end of the twentieth and twenty-first centuries

G. Krinner · O. Magand · I. Simmonds ·
C. Genthon · J. -L. Dufresne

Abstract The aim of this work is to assess potential future Antarctic surface mass balance changes, the underlying mechanisms, and the impact of these changes on global sea level. To this end, this paper presents simulations of the Antarctic climate for the end of the twentieth and twenty-first centuries. The simulations were carried out with a stretched-grid atmospheric general circulation model, allowing for high horizontal resolution (60 km) over Antarctica. It is found that the simulated present-day surface mass balance is skilful on continental scales. Errors on regional scales are moderate when observed sea surface conditions are used; more significant regional biases appear when sea surface conditions from a coupled model run are prescribed. The simulated Antarctic surface mass balance increases by 32 mm water equivalent per year in the next century, corresponding to a sea level decrease of 1.2 mm year^{-1} by the end of the twenty-first century. This surface mass balance increase is largely due to precipitation changes, while changes in snow melt and turbulent latent surface fluxes are weak. The temperature increase leads to an increased moisture transport towards the interior of the continent because of the higher moisture holding capacity of warmer air, but changes in atmospheric dynamics, in particular off the Antarctic coast, regionally modulate this signal.

G. Krinner (✉) · O. Magand · C. Genthon
LGGE, CNRS/UJF Grenoble, BP 96,
38402 St Martin d'Hères Cedex, France
e-mail: krinner@ujf-grenoble.fr

I. Simmonds
School of Earth Sciences, University of Melbourne,
Parkville, Victoria 3052, Australia

J. -L. Dufresne
LMD/IPSL, CNRS/Université Paris 6, Boîte 99,
75252 Paris Cedex 05, France

1 Introduction

The regional expression of global climate change tends to be stronger in polar regions than over the rest of the globe. This polar amplification has been evidenced on multiple time scales, e.g., glacial–interglacial (e.g., Cuffey et al. 1997; EPICA Project Members 2004) and centennial (e.g., Moritz et al. 2002), and many general circulation models predict it for the near future (Masson-Delmotte et al. 2006). It has been shown to be due to a general increase of poleward heat transport with increasing global mean temperature (Alexeev et al. 2005), with further amplification through local feedbacks (Holland and Bitz 2003). Furthermore, surface temperature changes in polar regions, in particular Antarctica, are amplified compared to changes aloft by the fact that the ubiquitous surface inversion strength is negatively correlated to air temperature (Phillpot and Zillman 1970). Concerning the recent decades, however, Antarctic temperature changes are not unambiguous. On one hand, a rapid and strong warming is observed over the Antarctic Peninsula (Vaughan et al. 2003) and in the mid-troposphere in winter (Turner et al. 2006); on the other hand, Doran et al. (2002) have reported a cooling trend on the East Antarctic coast in recent decades. Gillet and Thompson (2003) and Thompson and Solomon (2002)

showed that these contrasting trends can be explained by changes in the lower stratospheric and upper tropospheric dynamics caused by the destruction of the ozone layer over Antarctica. However, it has been shown that the changes in the Southern Annular Mode (SAM) leading to these contrasting temperature trends (Kwok and Comiso 2002) can also be explained by increased greenhouse gas concentrations (Fyfe et al. 1999; Kushner et al. 2001; Stone et al. 2001; Cai et al. 2003; Marshall et al. 2004). Concerning the Antarctic surface mass balance (SMB), these contrasting temperature trends are consistent with widespread glacier retreat on the Antarctic Peninsula over the past 50 years (Cook et al. 2005) and a decrease in the frequency of melt events over the last 20 years near the East Antarctic coast deduced from the satellite data (Torinesi et al. 2003). In the interior of the continent, a significant recent increase in the surface mass balance has been reported (Mosley-Thompson et al. 1998; Davis et al. 2005) and suggested to be a potential early indicator of anthropogenic climate change. However, model-based assessments of the Antarctic surface mass balance in recent decades (van de Berg et al. 2006; Monaghan et al. 2006) suggest statistically insignificant or slightly negative precipitation changes over the continent as a whole. Although mass loss of the totality of Earth's glaciers and ice sheets did play a major role in the sea-level rise of the recent decades (Miller and Douglas 2004), the contribution from recent Antarctic changes is thus difficult to assess. Moreover, although there is definitely a significant positive contribution to sea level rise of the mass balance of West Antarctica (Thomas et al. 2004), this might in part be due to changes in the ice dynamics, such as those observed after the collapse on the Larsen B ice shelf (de Angelis and Skvarca 2003). The ice shelf had previously been stable over several millennia (Domack et al. 2005), suggesting that this event might have been linked in turn to the recent strong warming over the Antarctic Peninsula, which leads to particularly high melt rates in summers with strong ''warm'' circulation anomalies in the area (Turner et al. 2002; van den Broeke 2005). Similarly, a surface melt increase can accelerate basal sliding via a better lubrication by water at the ice/rock interface, and can thus induce a more negative overall mass balance of an ice sheet, as shown by Zwally et al. (2002) for the case of Greenland.

If climate change accelerates in the coming century, the subsequent Antarctic surface mass balance (SMB) change might become more obvious, and its impact on global sea level might thus become substantial. This motivated climate model studies of the future surface mass balance of Antarctica (e.g., Thompson and Pollard 1997; Wild et al. 2003; Huybrechts et al. 2004). A major problem of these studies is the fact that, even at T106 resolution (about 110 km), the steep and narrow ablation zone at the margin of the ice sheets cannot be properly resolved. However, as stated by Wild et al. (2003), this problem is less acute for Antarctic than for Greenland SMB studies, because surface melt at the margin of the Antarctic continent is not very significant, even in a $2 \times CO_2$ climate. Nevertheless, even in the absence of significant melting, high resolution is still a prerequisite for credible simulations of the Antarctic surface mass balance, because the climate is strongly determined by the ice sheet topography, in particular near the steep margins (Krinner and Genthon 1997; Krinner et al. 1997a, b). The observed SMB exhibits a strong gradient near the coast because precipitation sharply decreases towards the interior (Vaughan et al. 1999). This gradient is obviously linked to: (1) orographic precipitation on the slopes of the ice sheet margin; (2) increasing distance to the oceanic moisture sources; and (3) a strong temperature gradient towards the interior of the continent, leading to low temperature on the plateau regions and thus to a low saturation vapour pressure. The interior of the Antarctic continent is therefore extremely dry, with annual precipitation below 50 mm water equivalent. In this extreme environment, ''intense'' precipitation events tend to occur when strong cyclone/anticyclone couples off the coast push moist air masses towards the interior (Bromwich 1988; Krinner and Genthon 1997). However, it is unclear whether these particular events bring the bulk of the precipitation in the interior of the continent, as some climate models (e.g., Noone and Simmonds 1998; Noone et al. 1999) and measurements in Dronning Maud Land (Reijmer et al. 2002) tend to suggest, or whether quasi-continuous extremely light fallout of ice crystals yields most of the precipitation total, as suggested by Ekaykin et al. (2004) for Vostok and observations reported by Bromwich (1988) for Plateau station. In fact, even the seasonality of precipitation is unknown in large parts of Antarctica because the small precipitation amounts are not measurable.

Here we present simulations of the Antarctic climate for the periods 1981–2000 and 2081–2100. The simulations were carried out with a global climate model with regionally high resolution over Antarctica (60 km). We first assess the quality of the simulated present-day SMB by comparing with available data. Simulated future changes in Antarctic SMB are then presented and analysed with respect to the precipitation-generating meteorological situations.

2 Methods

We used the LMDZ4 atmospheric general circulation model (Hourdin et al. 2006) which includes several improvements for the simulation of polar climates as suggested by Krinner et al. (1997b). The model was run with 19 vertical levels and 144×109 (longitude times latitude) horizontal grid points. These are regularly spaced in longitude and irregularly spaced in latitude. The spacing is such that the meridional grid-point distance is about 60 km in the region of interest southwards of the polar circle. Due to the convergence of the meridians, the zonal grid-point distance becomes small near the pole (80 km at the polar circle and below 60 km south of 77°S) in spite of the relatively low number of zonal grid points. The grid-stretching capability of LMDZ4 allows high-resolution simulations of polar climate at a reasonable numeric cost (e.g., Krinner and Genthon 1998; Krinner et al. 2004). Figure 1a shows the surface topography of the Antarctic continent as represented in the model at this resolution. Among the processes directly determining the ice sheet surface mass balance, the model simulates precipitation, turbulent latent energy surface fluxes (i.e., sublimation, evaporation, condensation and deposition), and snow or ice melt. However, it does not include a parameterization of blowing snow, although this process can be important, particularly in coastal regions (Gallée et al. 2001; Frezzotti et al. 2004).

Two 21 years long simulations were carried out, one for the end of the twentieth century (henceforth S20) and one for the end of the twenty-first century (henceforth S21). Only the last 20 years of the simulations are analysed here, the first year being discarded as spin-up. According to Simmonds (1985), this is an appropriate spin-up time for an atmosphere-only model. The prescribed sea surface boundary conditions (sea ice concentration and sea surface temperature) were taken from IPCC 4th assessment report simulations (Dufresne et al. 2005) carried out with the IPSL-CM4 coupled atmosphere-ocean GCM (Marti et al. 2005). LMDZ4 is the atmospheric component of IPSL-CM4. The climate sensitivity of IPSL-CM4 for a doubling of the atmospheric CO2 concentration from pre-industrial values (3.7°C) is situated in the upper part of the range of coupled models of the 4th IPCC assessment report (Forster and Taylor 2006). The Antarctic polar amplification in IPSL-CM4 is 16%, that is, temperature change over Antarctica is 16% greater than that of the global mean. This situates the model close to the average of the 4th IPCC assessment report

models (Masson-Delmotte et al. 2006). For S20, we used the IPSL-CM4 output of the historic 20CM3 run (mean annual cycle of the years 1981–2000). For S21, we used the SRESA1B scenario run (mean annual cycle of the years 2081–2100). The prescribed change in annual mean sea ice concentration around Antarctica is displayed in Fig. 1b. The greenhouse gas concentrations (CO_2, CH_4, N_2O, CFC11, CFC12) in our simulations were fixed to the mean values for the corresponding periods used in the IPSL-CM4 runs (CO_2 concentration is 348 ppmv in S20 and 675 ppmv in S21). Ozone was kept constant in these simulations, although stratospheric ozone variations were reported to have influenced recent Antarctic temperature trends via a modulation of the Southern Annular Mode (SAM: Thompson and Solomon 2002; Gillet and Thompson 2003), and might continue to do so in the future. In this context, it is worth mentioning a modelling study by Shindell and Schmidt (2004) which suggests that the future ozone recovery could reduce the moderating effect of the SAM changes induced by ozone depletion, and thus lead to an increased future warming. However, the assertion that ozone variations are the primary cause of recent SAM (and thus surface temperature) changes is challenged by Marshall et al. (2004), who report on GCM simulations showing SAM changes that are consistent with observations and occur before the onset of stratospheric ozone depletion.

In addition, a 21-year simulation with observed mean sea ice fraction and sea surface temperature for the period 1979–1988 was carried out. This simulation (henceforth O20) allows to identify eventual biases in S20 induced by the use of sea surface conditions from the coupled climate model. Figure 1c shows that the prescribed monthly sea ice area in S20 has a fairly constant low bias of about 2 million km^2 compared to the observed extent used in O20. We deem this bias acceptable as a result of a coupled climate model run, in the sense that the realism of the simulated sea-ice extent corresponds to the present state of the art of coupled climate modelling. We have to rely on the assumption that the sea-ice changes simulated by the coupled model are well captured in spite of the underestimate of the present-day mean sea ice extent.

Ablation is calculated directly from the GCM output in the following way. Instead of contributing to runoff, a fraction f of the annual liquid precipitation and meltwater can refreeze near the surface when percolating into the cold snowpack. Based on Pfeffer et al. (1991), Thompson and Pollard (1997) proposed a parameterization that links f to the ratio of annual snow or ice melt (M) to snowfall (S):
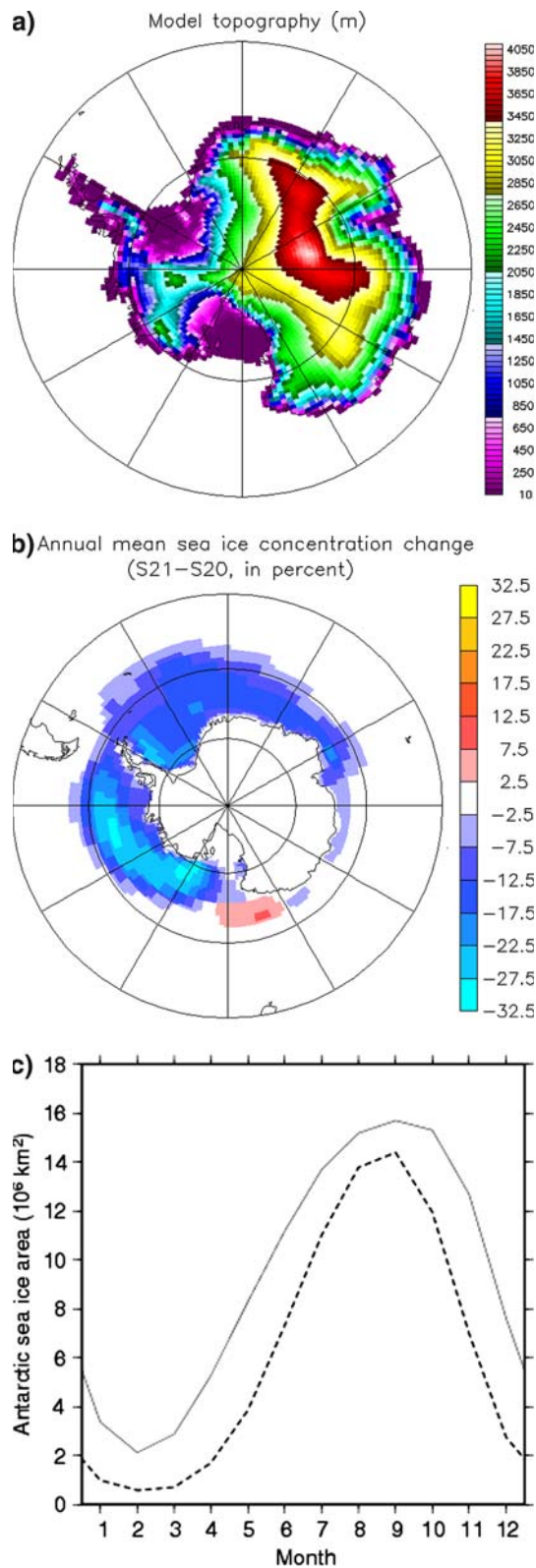
Fig. 1 Model configuration and boundary conditions. **a** Model topography of the Antarctic continent (m). **b** Annual mean sea ice concentration change (S21-S20, in percent). **c** Prescribed Antarctic Sea ice extent for the twentieth century simulations (*thin full line*: O20; *thick dashed line*: S20)

$$f = 1 - (M/S - 0.7)/(0.3).$$

Throughout this paper, SMB is therefore defined as

$$\text{SMB} = S + fR - E - (1 - f)M,$$

where R is the rainfall, and E represents sublimation. The term "sublimation" is used in the original sense of the word, that is, positive for the phase transformation from solid to gas. Deposition appears as negative sublimation in the model. The accumulation A is defined as

$$A = S + fR - E.$$

All these variables are calculated only for grid points with a minimum land ice fraction of 80%, as we are interested in the ice sheet mass balance only. This prevents a skewing of the results by taking into account ice sheet marginal grid points with a significant fraction of open ocean, sea ice or ice-free continental soil, which exist as a consequence of the mosaic surface scheme of LMDZ4.

Cyclonic activity off the Antarctic is analysed from GCM-simulated daily sea level pressure (p) with the objective cyclone tracking scheme of Murray and Simmonds (1991), with improvements described by Simmonds and Murray (1999) and Simmonds and Keay (2000). The scheme has been developed in particular to study southern hemisphere extratropical cyclones. The specific cyclone-related variables used here are the cyclone system density and average cyclone depth. System density is defined as the average number of centers of cyclonic depressions per unit area at a given time (for convenience, the unit area used to present the calculated system density here is one square degree of latitude, corresponding to approximately 12,000 km^2). In analogy to an axially symmetric paraboloidal depression of a given radius R on a flat field, the average depth of a cyclonic perturbation (in hPa) is calculated from the mean laplacian of the sea level pressure field over the radius of influence of the depression:

$$D = \frac{1}{4} \nabla^2 p \cdot R^2.$$

The radius of influence is determined by following lines of maximum negative gradient of $\nabla^2 p$ outwards from the cyclonic center until $\nabla^2 p$ becomes positive. For more details about the cyclone tracking scheme, the reader is referred to the papers cited above.

3 Simulated Antarctic SMB at the end of the twentieth century

Figure 2 displays the simulated Antarctic SMB for the years 1981–2000 from S20. The mean simulated SMB over the ice sheet is 151 kg m^{-2} year^{-1}. The respective values for total precipitation, sublimation, and melt are 164, 13, and 2 kg m^{-2} year^{-1}. The simulated mean accumulation on the ice sheet, 151 kg m^{-2} year^{-1}, falls within the range of observational estimates from 135 to 184 kg m^{-2} year^{-1} (Giovinetto et al. 1992; Yamazaki 1994). Apparent inconsistencies between the numbers given above are due to the parameterization of refreezing and rounding errors.

The individual components of the simulated SMB (precipitation, sublimation, and melt) are displayed in Fig. 3. Precipitation in S20 attains its maximum over coastal Mary Byrd Land (up to 1,525 kg m^{-2} year^{-1}), and secondary maxima are simulated over the Antarctic Peninsula (up to 1,025 kg m^{-2} year^{-1}) and along the East Antarctic Coast between 110°E and 150°E. Liquid precipitation is negligible. In simulation O20, which uses average observed instead of simulated sea surface conditions, the model yields stronger precipitation over the Antarctic Peninsula (up to 1,200 kg m^{-2} year^{-1}) and weaker precipitation over coastal Mary Byrd Land than in S20. As a consequence, the maximum precipitation in O20 is located over the Peninsula region, in agreement with large-scale estimates (Giovinetto and Bentley 1985; Vaughan et al. 1999), and the continental SMB is slightly higher than in S20 (162 kg m^{-2} year^{-1} compared to 151 kg m^{-2} year^{-1} in S20).

The simulated extent and location of Antarctic melt zones (Fig. 3c) is in very good agreement with satellite observations by Torinesi et al. (2003). The only notable

difference occurs over the Transantarctic Mountain Range near the Ross Sea and Ice Shelf, and this discrepancy could be explained by the fact that the GCM cannot resolve the small valley glaciers on which the melt occurs. Another possibility is that the satellite-deduced melt areas are in error in this mountainous region because rock outcrops lead to spurious melt signals (Mätzler 1987; Torinesi et al. 2003). In any case, using the parameterization of Thompson and Pollard (1997), we find that almost all the simulated meltwater refreezes, so that runoff is actually generated only on the northern part of the Antarctic Peninsula. This is in good agreement with a study by Listen and Winther (2005) based on observations and modeling. We obtain a similar extent of runoff areas when applying the temperature index method proposed by Ohmura et al. (1996), in which surface ablation is diagnosed when mean summer (DJF) temperatures, recalculated on a fine resolution grid with altitude-correction, exceed a prescribed threshold (–1.8°C). The total ablation is then calculated as $A = (514°C^{-1} T_{DJF} + 930)$ kg m^{-2} year^{-1} (equivalent to millimeter of water equivalent per year). Using high-resolution radar satellite topography (Bamber and Gomez-Dans 2006) and a –6°C/km summer temperature correction for altitude changes in Antarctic coastal regions (Krinner and Genthon 1999), this latter method also yields ablation only on the northern part of the Antarctic Peninsula.

Sublimation is negative over a large part of the interior of the continent. This means that the weak atmospheric turbulence in the generally stable boundary layer leads to ice crystal deposition over the plateau regions. However, the amount of mass deposited in this way generally does not exceed one tenth of the precipitation. Near the coast, sublimation becomes positive, and can represent a significant fraction (30%) of the precipitation in regions with strong winds along the East Antarctic coast. Similar to previous simulations (van den Broeke et al. 1997), the coastal sublimation has a clear maximum in summer, when the near-surface temperature inversion is weak, although the wind speeds are higher in winter. The continental mean sublimation is weakly positive, that is, the ice sheet loses mass to the atmosphere through turbulent latent heat fluxes.

We will now briefly compare the simulated SMB to reliable measurements and available large-scale estimates. Figure 4a displays the ratio between the simulated SMB in S20 and gridded estimates by Vaughan et al. (1999). Figure 4b displays the same ratio for simulation O20. The patterns of the positive and negative biases shown for S20 and O20 are similar, but the discrepancies are weaker in O20, which uses average
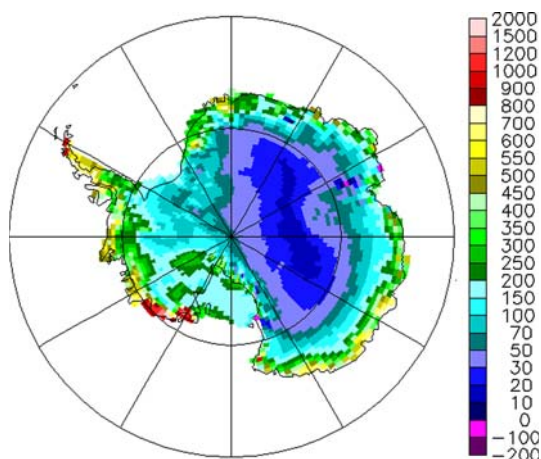

Fig. 2 Simulated Antarctic Ice Sheet SMB (kg m^{-2} year^{-1}) for the years 1981–2000

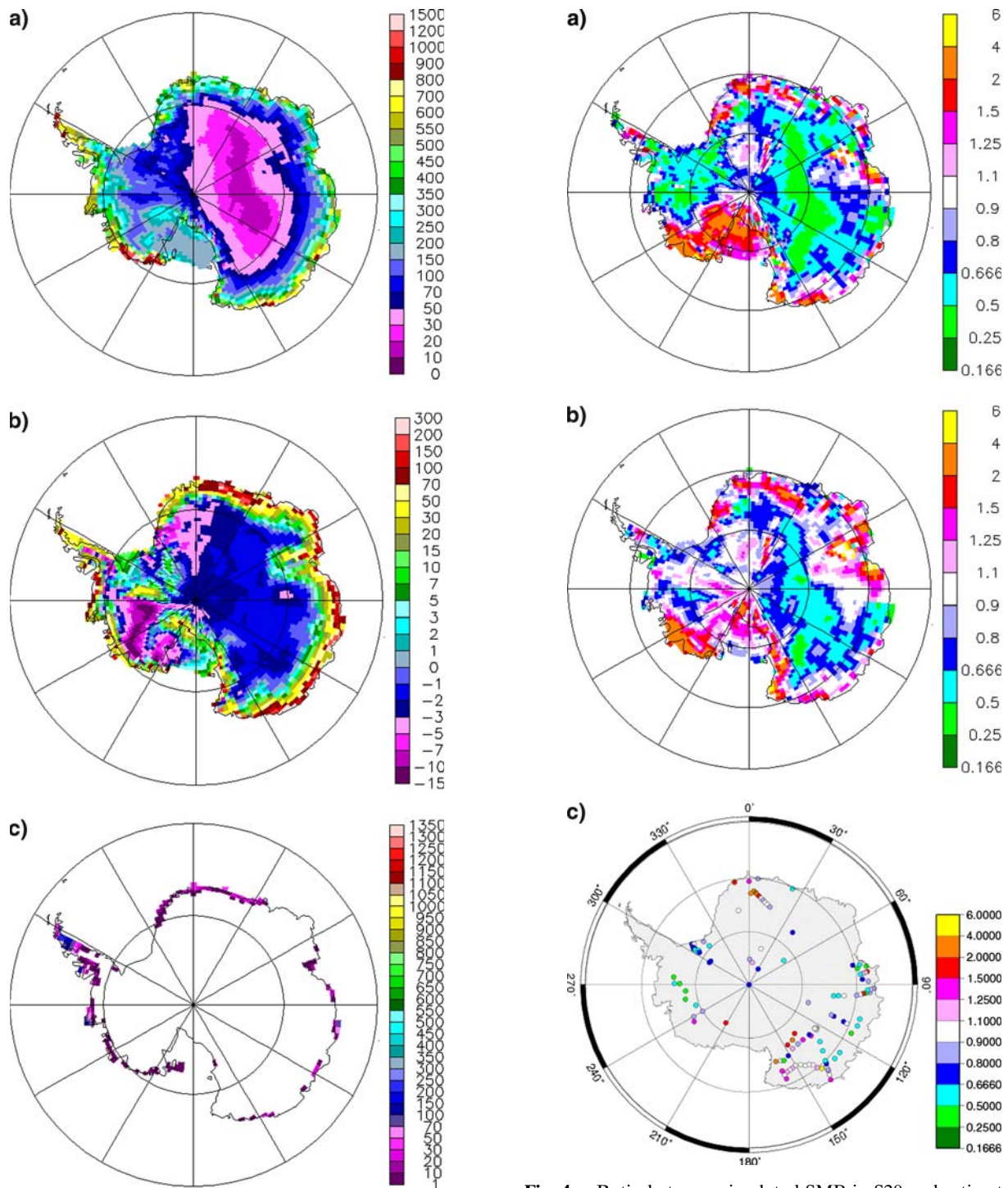**Fig. 3** Individual components of the simulated Antarctic Ice Sheet SMB (kg m^{-2} year^{-1}) for the years 1981–2000. **a** Precipitation; **b** sublimation; **c** melt

Fig. 4 a Ratio between simulated SMB in S20 and estimates by Vaughan et al. (1999); **b** ratio between simulated SMB in O20 and estimates by Vaughan et al. (1999); **c** ratio between simulated (S20) and observed SMB in selected Antarctic locations where reliable observations exist

observed sea surface conditions, than in S20, in which average simulated sea surface conditions are prescribed. In both simulations, strong positive biases appear in coastal Mary Byrd Land. Concerning this particular region, Genthon and Krinner (2001) showed that this is

a common bias shared by many high-resolution GCMs and reanalyses. They state that it is possible that, rather than the models, the gridded SMB estimates of Vaughan et al. (1999) are in error in this

area, because they are based on extrapolations from SMB measurements in the interior. Regional climate model simulations by van den Broeke et al. (2006) also suggest this. A large difference between the errors for S20 (Fig. 4a) and O20 (Fig. 4b) is the large bias dipole in West Antarctica in S20. The reason for this problem is the underestimated intensity of the Amundsen Sea low pressure zone in S20. As discussed by Genthon et al. (2005), a weaker Amundsen Sea low leads to increased precipitation over Mary Byrd Land and reduced precipitation to the East. These precipitation errors are absent in simulation O20, which uses observed sea surface conditions. The model misfit in S20 is thus due to errors in the sea surface conditions obtained from the coupled model run. An apparent negative bias both of S20 and O20 is located in central East Antarctica, essentially along the ridge of the ice sheet. Here, both simulations yield lower SMB than the gridded estimates of Vaughan et al. (1999) suggest. However, as will be shown in the following, this negative bias in central East Antarctica does not appear when the model simulations are compared to selected reliable measurements.

Figure 4c shows the ratio between simulated and observed SMB for selected locations in Antarctica in S20. Because of high interannual SMB variability on small spatial scales (Frezzotti et al. 2004, 2005; Magand et al. 2004), we selected locations where data represent at least a decade of SMB (Minikin et al. 1994; Smith et al. 2002; Pourchet et al. 2003; Magand et al. 2004; Kaspari et al. 2004; Frezzotti et al. 2004, 2005) to reduce as much as possible the effect of small-scale spatial and temporal variability and thus increase temporal and spatial representativeness of observed SMB values. This approach follows the recommendations by the ISMASS Committee (2004). Additionally, we used observed SMB data from the Dome F (Watanabe et al. 2003) and Siple Dome (Taylor et al. 2004) deep drilling sites. Furthermore, we excluded locations at which the model topography is in error by more than 300 m. Surprisingly few data points had to be dropped as a consequence of this criterion. Few clear and strong regional biases appear in the figure. In particular, the model does not show a particular bias in central East Antarctica, as the comparison to the gridded estimates tended to suggest; on the contrary, the simulated SMB agrees rather well with observed values from firn cores at the deep drilling sites Dome C, Dome F, and Vostok. One regional bias seems to consist in an underestimate of SMB in coastal Wilkes Land between 110 and 140°E, where the model simulates less than 66% of the observed values. Further west, the model seems to overestimate the

SMB, but the bias is not very strong. Around 77°S and 145°E, a group of three points indicating a strong overestimate of the SMB is linked to the presence of wind-glazed surfaces with extremely low accumulation rates due to sublimation of blowing snow (Frezzotti et al. 2002, 2004). This is a process that the model does not represent. Along an axis from Dome F (39.8°E, 77.3°S) via the South Pole to Siple Dome (148.8°W, 81.7°S), the model has a tendency to slightly underestimate the SMB. On smaller spatial scales, however, significant discrepancies exist. Interestingly, points with large under- and overestimates are often very close to each other. In such cases, the misfits are largely due to high spatial variability in the data on very short distances (Magand et al. 2004; Frezzotti et al. 2004, 2005), which cannot be sufficiently well represented in the model, leading to spuriously high apparent and localized biases in Fig. 4c. This is supported by the fact that the agreement between model and data is generally improved by using only the mean observed SMB of several data points at places where several data points correspond to one single model grid point. For instance, two firn core measurements at approximately 151.1°E and 74.8°S, at a few hundred meters from each other, indicate SMBs of 82 and 44 kg m^{-2} year^{-1}, respectively, with the simulated SMB (50 kg m^{-2} year^{-1}) lying between these values. Taking into consideration these problems linked to spatial heterogeneity of SMB, we conclude that on regional scales, SMB is typically represented to within about 20% of the true value by the GCM, except in regions where sublimation of blowing snow has a significant impact on SMB, and except in regions where the use of simulated sea surface conditions from a coupled model run leads to errors in the simulated patterns of atmospheric dynamics.

4 Simulated Antarctic SMB at the end of the twenty-first century

Figure 5 displays the simulated Antarctic SMB for the years 2081–2100. Mean simulated SMB over the ice sheet is 183 kg m^{-2} year^{-1}. The respective values for total precipitation, sublimation, and melt are 199, 15, and 7 kg m^{-2} year^{-1}.

Recent observed increases of SMB over central East Antarctica have been suggested to be a potential early indicator of anthropogenic climate change (Mosley-Thompson et al. 1998). Similar to other simulations of future Antarctic SMB (e.g., Wild et al. 2003), the simulations presented here confirm that
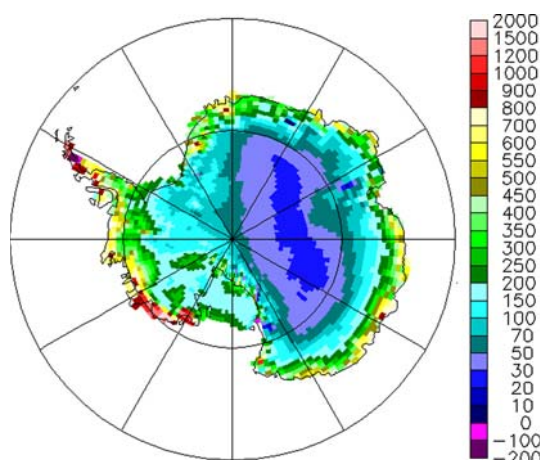
Fig. 5 Simulated Antarctic Ice Sheet SMB (kg m^{-2} year^{-1}) for the years 2081–2100, SRESA1B scenario

future accumulation is indeed greater over most of the interior of the continent. The physical mechanism underlying this effect on the continental scale appears to be the increased moisture holding capacity of the air at higher temperatures. However, the model also simulates drying in some regions, such as the interior of Mary Byrd Land or Wilkes Land (see Fig. 6, which shows the ratio between the annual mean precipitations of S21 and S20). In spite of regional drying, though, the continental mean precipitation increases by 21%. Because the low-lying coastal regions have much higher mean precipitation rates than the interior, the continental-mean precipitation increase is dominated by the coastal areas. The spatially integrated precipitation increase over the grid points
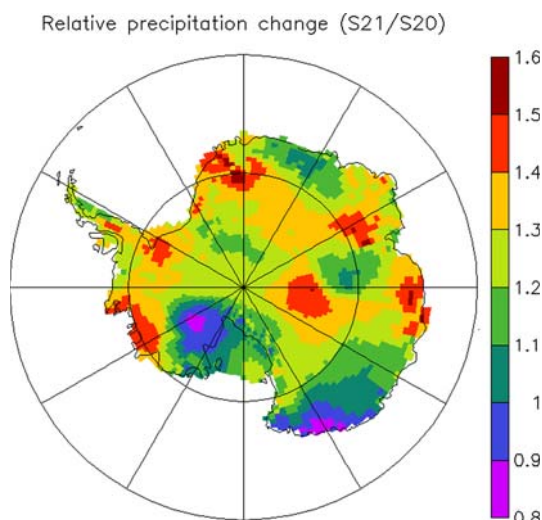
below 1,500 m is twice that of the grid points above 1,500 m, although the total Antarctic surface area above 1,500 m is almost twice the area below 1,500 m. Because the precipitation patterns are strongly determined by topographical features, the continental-scale pattern of precipitation in S21 is very similar to that of S20, even in sub-regional details. Rainfall becomes a significant part (locally up to 30%) of total annual precipitation at the tip (northernmost 250 km) of the Antarctic Peninsula. Elsewhere, it generally remains negligible.

Simulated total snow and ice melt over Antarctica increases by more than a factor of three (from 2 in S20 to 7 kg m^{-2} year^{-1} in S21), but it still remains small compared to the total precipitation. Regionally, though, the increased melt is important, particularly over the Antarctic Peninsula, where several grid points with negative SMB exist in S21, due to high melt rates of up to 800 kg m^{-2} year^{-1}. As in S20, this northern part of the Peninsula is the only region where the melted snow does not refreeze, but is lost as runoff. Of the continental mean meltwater (7 kg m^{-2} year^{-1}), almost 80% is diagnosed to refreeze even at the end of the twenty-first century. Patterns of latent turbulent surface fluxes in S21 are very similar to that of S20, with deposition in the interior (but slightly less than in S20), and sublimation in the coastal regions.

The Antarctic SMB increase of + 32 kg m^{-2} year^{-1} from S20 to S21 corresponds to a net sea level decrease of 1.2 mm year^{-1} by the end of the twenty-first century, compared to the end of the twentieth century.

5 Characteristics of present and future precipitation

5.1 Seasonality

Figure 7 displays the simulated monthly mean total precipitation and snowfall time series for the Antarctic Plateau, the east Antarctic coastal area, the Antarctic Peninsula, and the interior of Mary Byrd Land. The early winter maximum of simulated east Antarctic coastal precipitation in S20 is replaced by a broader winter maximum in S21, but most importantly, the summer minimum is much less pronounced in S21 than in S20. Over the plateau regions above 3,000 m altitude, the precipitation increase is more equally distributed over the year. The present-day autumn precipitation maximum in the interior of Mary Byrd Land is replaced by a winter maximum in S21. This particular feature will be discussed in subsection "Sea ice cover, cyclonicity and precipitation".
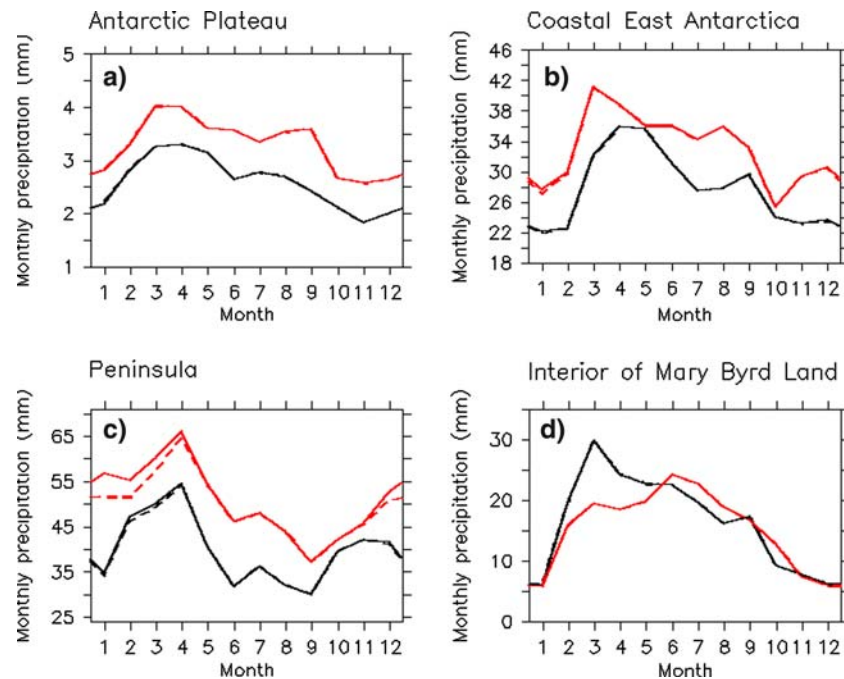

Fig. 6 Relative annual mean precipitation change on the Antarctic Ice Sheet (S21/S20)

Fig. 7 Simulated monthly mean precipitation (kg m^{-2} month^{-1}) for the periods 1981–2000 (*black*) and 2081–2100 (*red*), for different Antarctic regions. *Full lines*: Total precipitation; *dashed lines*: snowfall. Total precipitation and snowfall are almost indistinguishable except on the Peninsula. The Antarctic Plateau includes all grid points above 3,000 m altitude. Coastal East Antarctica includes all grid points below 2,000 m altitude, at longitudes between 30°W and 180°E, and north of 78°S in order to exclude shelf areas. The Peninsula region is defined as the area north of 75°S, at longitudes between 80°W and 50°W. The interior of Mary Byrd Land is the region between 80 and 85° south and between 150 and 120° west

5.2 Link between mean circulation, temperature, and precipitation changes

Obvious features of the prescribed change in annual mean sea ice concentration from S20 to S21 (Fig. 1b) are a sea ice concentration increase of Wilkes Land, and a strong concentration decrease further East, in the Ross and Amundsen Seas. It is interesting to note that this pattern is similar to the recent observed spatial pattern of sea ice edge trends, linked to an increase of the positive polarity of the Southern Annular Mode (SAM) as shown by Kwok and Comiso (2002). Indeed, the Antarctic Oscillation Index, defined as the normalized zonal sea level pressure difference between 40°S and 65°S (Gong and Wang 1999), is higher in S21 than in S20. As stated in the introduction, this is consistent with many studies of the impact of enhanced greenhouse gas concentrations on the southern hemisphere circulation patterns (Fyfe et al. 1999; Kushner et al. 2001; Stone et al. 2001; Cai et al. 2003; Marshall et al. 2004). In a manner that is coherent with the impact on sea ice, positive phases of the SAM lead to a warming over the Antarctic Peninsula and a cooling (or a weaker warming in a global change context) over East

Antarctica (Kwok and Comiso 2002). Precipitation in high latitudes is often limited by the low water holding capacity of cold air. The precipitation reduction in Wilkes Land simulated by LMDZ4 is therefore not too surprising. Of course, modifications in the mean state of the Southern Annular Mode could also influence factors other than air temperatures, such as moisture source regions, but here we focus on the link between temperature and precipitation. In this respect, it is worth noting that the relative precipitation change shown in Fig. 6 shows some striking similarities to the relative precipitation change simulated by the ECHAM4 model (Huybrechts et al. 2004).

We will now analyse the link between precipitation and temperature changes in some more detail. Following the water holding capacity argument, one can expect a roughly exponential link between temperature and precipitation changes over Antarctica (e.g., Robin 1977). Strictly speaking, the pertinent temperature in this case is not the annual mean temperature, but the temperature during the months when precipitation preferentially falls. Following Krinner et al. (1997a) and Krinner and Werner (2003), we therefore introduce the precipitation-weighted temperature T_{pr}, defined as

$$T_{\mathrm{pr}} = \sum (T_i P_i) / \sum P_i$$

where T_i and P_i indicate monthly mean surface air temperature and precipitation, and the sums are calculated over the 12 months of the simulated mean annual cycle. Figure 8 displays the simulated temperature changes (S21–S20) and precipitation-weighted temperature changes (S21–S20). On subcontinental scales, no link is apparent between the annual mean temperature change (Fig. 8a) and the relative precipitation change (Fig. 6). Conversely, there is a fairly clear, though less than perfect, match between the relative precipitation change and the change in precipitation-weighted temperature (Fig. 8b). In regions where T_{pr} increases only slightly, precipitation does not increase or even decreases, while strong precipitation increases tend to be linked to strong T_{pr} increases. This is interesting, as it indicates that the link between precipitation and temperature changes is not as simple as often assumed in ice core studies, in particular in ice core dating exercises, where a fixed relationship between mean annual temperature and accumulation, and changes thereof, is commonly assumed (e.g., Parrenin et al. 2004). However, this issue is beyond the scope of the present study. In any case, the fact that the patterns in Figs. 6 and 8b do not match perfectly indicates that other processes also influence the precipitation changes in Antarctica. These will be analysed in the following.
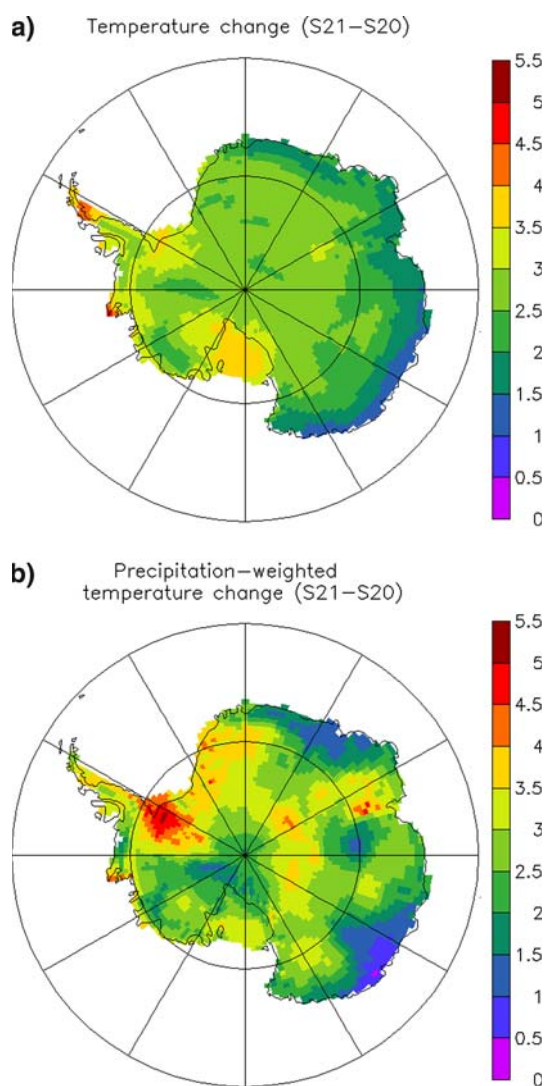
5.3 Sea ice cover, cyclonicity and precipitation

Watkins and Simmonds (1995) have shown that an intimate synoptic connection exists between sea ice and cyclone behaviour, which gives rise to the general relationship between Antarctic Sea ice concentration and cyclonicity reported by Simmonds and Wu (1993). Following these findings, the simulated changes in cyclonic system density (Fig. 9) are consistent with the sea ice concentration changes displayed in Fig. 1b. Off Wilkes Land, the increased sea ice concentration reduces the local moisture source and weakens the cyclonic systems, both effects leading to reduced precipitation shown in Fig. 6, and thus adding to the effects of the mean circulation and temperature changes discussed in the previous section.

Again in agreement with the findings of Simmonds and Wu (1993), decreased sea ice concentration along the Antarctic Peninsula in the Weddell Sea in S21 leads to increased lee cyclogenesis, and thus to increased system density, in this area. This strengthened cyclonic circulation over the Weddell Sea induces a strong precipitation increase on Coates Land in S21, contrary to the region south of the Filchner/Ronne Ice Shelf, which is more exposed to outflow of cold air from the East Antarctic Plateau.

The situation is different in the interior of Mary Byrd Land, where precipitation decreases in S21 compared to S20 (Fig. 6). The precipitation reduction is essentially due to a substantial precipitation reduction during the autumn months, particularly in March, as can be seen in Fig. 7d. For the present, the model simulates a clear precipitation maximum during these months in the interior of Mary Byrd Land, while this maximum disappears in S21. This is due to sea level pressure differences between S21 and S20 in the Amundsen Sea off Mary Byrd Land, as can be seen in
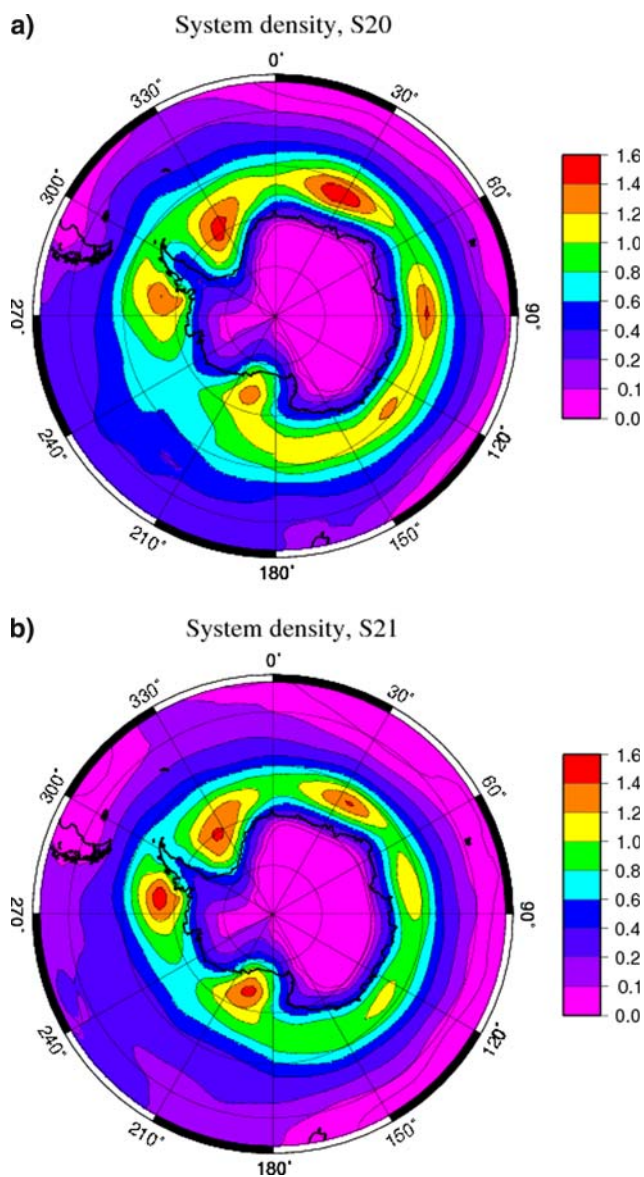

Fig. 8 Link between temperature and precipitation changes on the Antarctic Ice Sheet. **a** Simulated annual mean surface air temperature change (S21-S20, °C); **b** simulated change of annual mean precipitation-weighted surface air temperature (S21-S20, °C)

a) System density, S20

b) System density, S21

Fig. 9 Simulated mean density of cyclonic systems $(10^{-3}/(°lat)^2)$. **a** 1981–2000 (S20); **b** 2081–2100 (S21)

Fig. 10 Simulated sea-level pressure difference (hPa) between S21 and S20 in march

Fig. 10. The decrease in autumn sea level pressure over the Amundsen Sea in S21, linked to the sea-ice concentration decrease shown in Fig. 1b, strengthens the flow of cold and dry air masses from the top of the West Antarctic Ice Sheet across the interior of Mary Byrd Land. Closer to the coast, the increased annual mean cyclonic activity (Fig. 9) does induce a strong annual mean precipitation increase. In this context, it is noteworthy that a maximum of climate variability exists in the Amundsen and Bellingshausen Seas, due to the asymmetric nature of the orography in Antarctica (Lachlan-Cope et al. 2001a). In some cases, this variability seems to be excited by ENSO (e.g., Genthon and Cosme 2003; Fogt and Bromwich 2006),
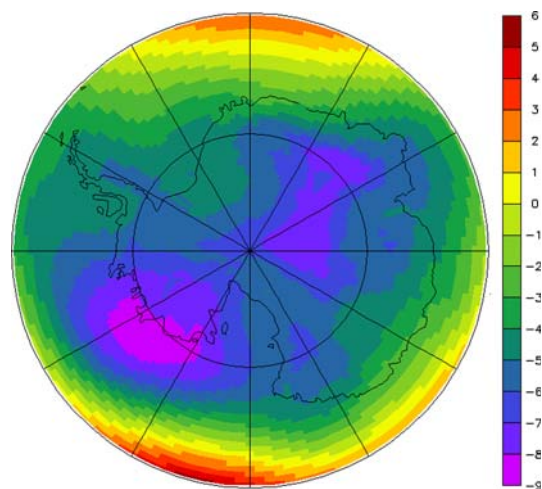
but the observed variability, which climate models tend to reproduce fairly correctly, "has a white spectrum consistent with random forcing by weather events and a decoupling from oceanic integration" (Connolley 1997). Given, in addition, that the prescribed sea surface conditions in our simulations have no interannual variability, and that no clear El-Niño type signal exists in either the prescribed tropical mean SST changes in our model runs or in the simulated sea level pressure pattern changes over the South Pacific, a modified ENSO forcing can be ruled out as cause for the precipitation changes in West Antarctica simulated in this model.

5.4 Intensity of individual precipitation events

Additional insight into the characteristics of precipitation events can be gained by analyzing the intensity of individual precipitation events. Figure 11 displays the number of days per year with daily precipitation exceeding five times the mean daily precipitation for the corresponding simulation ("NP5" in the following). The threshold value for a precipitation event to be classified as "intense" therefore depends on the mean precipitation at each point, and varies between S20 and S21. NP5 is tightly linked to the model topography. For the present (Fig. 11a), NP5 attains minimum values of only 4 days per year on the ridge of the East Antarctic Plateau, and regional minima systematically over other ice sheet domes and ridges, and on mountain chains (e.g., on the Peninsula). Maximum values of NP5 are attained in coastal East Antarctica, coastal Mary Byrd Land, and on the flat major shelves (Ross and Filchner/Ronne). In these areas, daily precipitation exceeds five
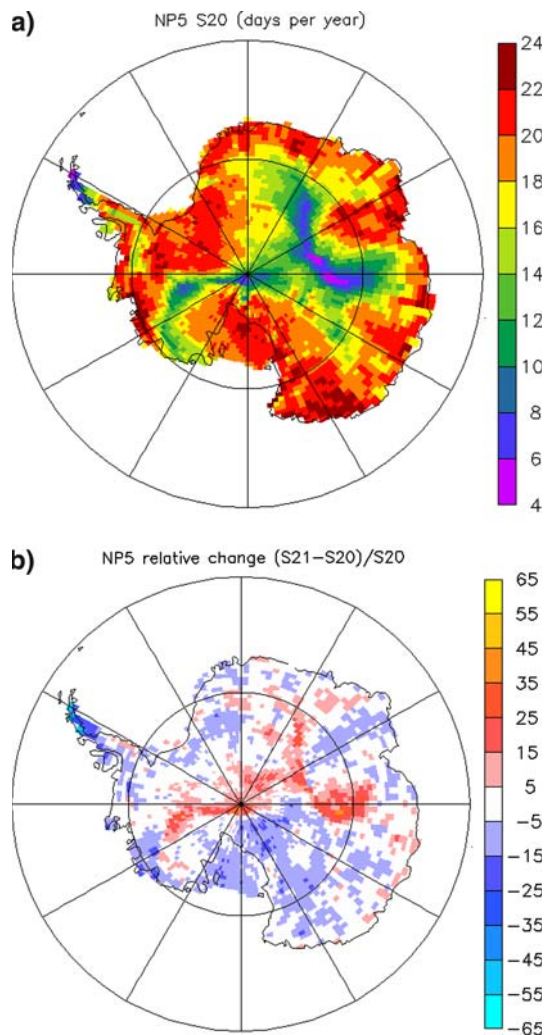
Fig. 11 Number of days with precipitation exceeding five times the annual daily mean (NP5). **a** Present day (S20); **b** relative change from the end of the twentieth to the end of the twenty-first century (S21-S20, in percent)

frequent and light clear sky precipitation ("diamond dust") is thought to deliver the major part of total precipitation in the remote interior (e.g., Bromwich 1988; Lachlan-Cope et al. 2001b), but blocking-high activity in the Southern Ocean can occasionally cause oceanic air masses to intrude far into the interior and lead to significant precipitation, as for example during the 2001/2002 summer season at Dome C (Massom et al. 2004). The low values of NP5 over the Antarctic Peninsula, however, are linked to the high frequency of cyclonic perturbations around this area (Fig. 9a), leading to high annual mean precipitation (Fig. 3a) delivered by many more or less equally strong precipitation events, and is consistent with observations (Turner et al. 1995; Russell et al. 2004). The pattern of NP5 for simulation S21 (not shown) is very similar to that for S20. The relative change of NP5 from S20 to S21 (Fig. 11b) indicates that the number of relatively strong precipitation events near the ice sheet domes and ridges, in particular in central East Antarctica, increases. Because the mean precipitation increases from S20 to S21, this also means that the frequency of strong precipitation events in the interior would be found to increase if, in the definition of what such an intense event is, the same numeric value of the threshold was used in S20 and S21. This indicates an increased frequency of intrusions of moist marine air, in spite of a lower future cyclonic system density. These apparently conflicting findings can be reconciled by recognizing that the intensity of the simulated cyclonic systems off the East Antarctic Coast, measured as the depth of the cyclonic depression in hPa of sea level pressure, increases from about 10 hPa in S20 to about 12 hPa in S21 (not shown). In other words, although the model suggests that there will be less cyclones off the East Antarctic coast in the future, the remaining cyclones will carry oceanic moisture further inland.

6 Concluding summary and discussion

The present-day Antarctic surface mass balance, as simulated by the LMDZ4 AGCM at a resolution of about 60 km over large parts of the continent, is in good agreement with continental-scale estimates. On regional scales, biases of about 20% appear when observed sea surface conditions are prescribed as boundary condition. The use of sea surface conditions from a coupled model run regionally induces larger biases. Such problems could be avoided by constructing sea surface boundary conditions for the twenty-first

times the mean daily precipitation on 20 days or more, indicating that frequent and strong cyclones off the coast bring the bulk of the annual total precipitation, as indicated by observations (Bromwich et al. 1988). In agreement with measurements in the interior of Dronning Maud Land (around 75°S, 0°E) by Reijmer et al. (2002), simulated NP5 is fairly high in this region. Conversely, on the plateau regions, and particularly on the ridges and domes, precipitation is more evenly distributed in time. This does not mean that there cannot be a distinct seasonality (see Fig. 7), but it indicates that precipitation tends to fall in relatively smaller amounts and on more frequent occasions. Because the precipitation amounts on the central Antarctic Plateau are so tiny, reliable measurements of the intensity of particular events do not exist. Fairly

century with an anomaly method using present-day observed sea surface conditions and coupled model anomalies. However, such anomaly methods can be problematic because the different aspects of the simulated climate change (such as the amplitude of the latitudinal shift of the sea ice edge, total sea ice area variations, sea surface temperature change, and regional differences in these changes) usually cannot all be reproduced in a faithful and meaningful way in the constructed forcing field. In this study, we therefore chose to use the sea surface conditions from the coupled IPCC model run directly. On local scales, the SMB biases can be rather large, but we suspect that high fine scale spatial variability, which cannot be captured by the model, leads to low representativeness of many point measurements. In some regions, model-data misfits seem to be due to the missing representation of the sublimation of blowing snow. This process should be taken into account in future versions of the model. The results we obtain indicate that realistic estimates of Antarctic surface melt and the induced mass loss can be obtained by using the surface melt that is directly simulated by the model and applying a parameterization of refreezing of surface water. This approach leads to a very low estimated mass loss through surface melt, both in present-day and future (end of the twenty-first century) conditions. The spatial resolution used in these simulations seems sufficient for a reasonable assessment of the continental and regional scale surface mass balance in Antarctica. It remains to be seen whether this direct approach at similar resolution can be applied to Greenland, where melt on the margins of the ice sheet is much more intense.

The model suggests an Antarctic surface mass balance (SMB) increase of $+ 32$ kg m^{-2} year^{-1} from within the 100 years from 1981–2000 to 2081–2100, corresponding to a net sea level decrease of 1.2 mm year^{-1} by the end of the twenty-first century. This is the same as the value obtained by Wild et al. (2003) with the ECHAM4 GCM at about 100 km horizontal resolution. However, the numbers cannot be compared strictly because Wild et al. (2003) simulate the climate change between the present and the approximate time of CO_2 concentration doubling with respect to pre-industrial values (which occurs around 2060 in the SRES A1B scenario used as a basis for our simulations). In a study using a regional climate model at 55 km resolution, van Lipzig et al. (2002) prescribed a 2°C temperature increase at the sea surface and the lateral boundaries around Antarctica, while keeping constant the relative humidity at the lateral boundaries. This increased humidity transport towards the Antarctic leads to a 30% increase of the continental-scale SMB. The experiment by van Lipzig et al. (2002) is of course not easily compared with ours, but given the approximate temperature increase of about 3°C in our simulations, and a concomitant SMB (and precipitation) increase of about 21%, it appears that the SMB sensitivity obtained by van Lipzig et al. (2002) is clearly stronger than what is suggested by our model. It is also stronger than the SMB sensitivities reported by Huybrechts et al. (2004) for the ECHAM4 and HadAM3H models, because these are close to the value obtained with LMDZ4. In this respect, it is noteworthy that the 2°C warming prescribed by van Lipzig et al. (2002) at the lateral boundaries of their model, typically around 55°S, roughly corresponds to the tropospheric temperature increase simulated by LMDZ4 in this region, the prescribed sea surface temperature increase in the region being somewhat weaker.

If we suppose that the change in SMB simulated by LMDZ4 is linear in the next 100 years, this SMB increase would lead to a cumulated sea level decrease of about 6 cm. However, it is clear that changes in glacier dynamics, particularly in West Antarctic ice streams, might have important impacts on future sea level changes. These changes in glacier dynamics might be caused by an increased surface melt in low-lying areas of Antarctica, although the model indicates that the overwhelming part of the meltwater will refreeze also at the end of the twenty-first century. Future surface mass balance changes in Antarctica can thus essentially be traced back to precipitation changes. Although there is a continental-scale increase of precipitation going along with a continental-scale warming, the link between precipitation and temperature change is more complicated than often assumed. Changes in atmospheric dynamics, largely influenced by sea-ice changes, modulate this relationship on regional scales. Moreover, the seasonality of precipitation and temperature, and changes thereof, are important parameters that have to be taken into account in the analyses of this relationship. In the interior of Antarctica, precipitation increases roughly equally at all seasons, while in coastal regions, the signal is more complicated and spatially variable. The simulated increase (decrease) of cyclonic system density in West (East) Antarctica seems to be an important factor in these changes. In the interior of the continent, intrusion of marine air masses pushed by powerful coastal weather systems becomes more frequent, because the mean intensity of coastal cyclones off the East Antarctic coast increases.

References

Alexeev VA, Langen PL, Bates JR (2005) Polar amplification of surface warming on an aquaplanet in "ghost forcing" experiments without sea ice feedbacks. Clim Dyn 24:655–666

de Angelis H, Skvarca P (2003) Glacier surge after ice shelf collapse. Science 299:1560–1562

Bamber JL, Gomez-Dans JL (2006) The accuracy of digital elevation models of the Antarctic continent. Earth Planetary Sci Lett 237:516–523

Bromwich D (1988) Snowfall in high southern latitudes. Rev Geophys 26:149–168

Cai W, Whetton PH, Karoly DJ (2003) The response of the Antarctic oscillation to increasing and stabilized atmospheric CO_2. J Clim 16:1525–1538

Connolley WM (1997) Variability in annual mean circulation in southern high latitudes. Clim Dyn 13:745–756

Cook AJ, Fox AJ, Vaughan DG, Ferrigno JG (2005) Retreating glacier fronts on the Antarctic Peninsula over the past half-century. Science 308:541–544

Cuffey K, Clow GD, Alley RB, Stuiver M, Waddington E, Saltus R (1997) Large Arctic temperature change at the Wisconsin-Holocene deglacial transition. Science 270:455–458

Davis CH, Li Y, McConnell JR, Frey MM, Hanna E (2005) Snowfall-driven growth in East Antarctic Ice Sheet mitigates recent sea-level rise. Science 308:1877–1878

Domack E, Duran D, Leenter A, Ishman S, Doane S, McCallum S, Amblas D, Ring J, Gilbert R, Prentice M (2005) Stability of the Larsen B ice shelf on the Antarctic Peninsula during the Holocene epoch. Nature 436:681–685

Doran PT, Priscu JC, Lyons WB, Walsh JE, Fountain AG, McKnight DM, Moorhead DL, Virginia RA, Wall DH, Clow GD, Fritsen CH, McKay CP, Parsons AN (2002) Antarctic climate cooling and terrestrial ecosystem response. Nature 415:517–520

Dufresne JL, Quaas J, Boucher O, Denvil S, Fairhead L (2005) Contrasts in the effects on climate of anthropogenic sulfate aerosols between the 20th and the 21st century. Geophys Res Lett 32:L21703. DOI 10.1029/2005GL023619

Ekaykin AA, Lipenkov VY, Kuzmina IN, Petit JR, Masson-Delmotte V Johnsen SJ (2004) The changes in isotope composition and accumulation of snow at Vostok station over the past 200 years. Ann Glaciol 39:569–575

EPICA Project Members (2004) Eight glacial cycles from an Antarctic ice core. Nature 429:623–628

Fogt RL, Bromwich DH (2006) Decadal variability of the ENSO teleconnection to the high latitude South Pacific governed by coupling with the Southern Annular Mode. J Clim 19:979–997

Forster PM, Taylor KE (2006) Climate forcings and climate sensitivities diagnosed from coupled climate model integrations. J Clim (in press)

Frezzotti M, Gandolfi S, La Marca F, Urbini S (2002) Snow dunes and glazed surfaces in Antarctica: new field and remote-sensing data. Ann Glaciol 34:81–88

Frezzotti M, Pourchet M, Flora O, Gandolfi S, Gay M, Urbini S, Vincent C, Becagli S, Gragnani R, Proposito M, Severi M, Traversi R, Udisti R, Fily M (2004) New estimations of precipitation and surface sublimation in East Antarctica from snow accumulation measurements. Clim Dyn 23:803–813

Frezzotti M, Pourchet M, Flora O, Gandolfi S, Gay M, Urbini S, Vincent C, Becagli S, Gragnani R, Proposito M, Severi M, Traversi R, Udisti R, Fily M (2005) Spatial and temporal variability of snow accumulation in East Antarctica from traverse data. J Glaciol 172:113–124

Fyfe JC, Boer GJ, Flato GM (1999) The Arctic and Antarctic oscillations and their projected changes under global warming. Geophys Res Lett 26:1601–1604

Gallée H, Guyomarc'h G, Brun E (2001) Impact of snow drift on the Antarctic Ice Sheet Surface Mass Balance: possible sensitivity to snow-surface properties. Boundary Layer Meteorol 99:1–19

Genthon C, Kaspari S, Mayewski PA (2005) Interannual variability of the surface mass balance of West Antarctica from ITASE cores and ERA40 reanalyses, 1958–2000. Clim Dyn 24:759–770

Genthon C, Krinner G (2001) Antarctic surface mass balance and systematic biases in general circulation models. J Geophys Res 106:20653–20664

Genthon C, Cosme E (2003) Intermittent signature of ENSO in West-Antarctic precipitation. Geophys Res Lett 30: 2081. DOI 10.1029/2003GL018280

Giovinetto MB, Bentley CR (1985) Surface balance in ice drainage systems of Antarctica. Antarct J US 20:6–13

Giovinetto MB, Bromwich DH, Wendler G (1992) Atmospheric net transport of water vapor and latent heat across 70°S. J Geophys Res 97:917–930

Gillet NP, Thompson DWJ (2003) Simulation of recent southern hemisphere climate change. Science 302:273–275

Gong D, Wang S (1999) Definition of Antarctic oscillation index. Geophys Res Lett 26:459–462

Holland MM, Bitz CM (2003) Polar amplification of climate change in coupled models. Clim Dyn 21:221–232

Hourdin F, Musat I, Bony S, Braconnot P, Codron F, Dufresne JL, Fairhead L, Filiberti MA, Friedlingstein P, Grandpeix JY, Krinner G, Le Van P, Li ZX, Lott F (2006) The LMDZ4 general circulation model: climate performance and sensitivity to parametrized physics with emphasis on tropical convection. Clim Dyn (in press)

Huybrechts P, Gregory J, Janssens I, Wild M (2004) Modelling Antarctic and Greenland volume changes during the 20th and 21st centuries forced by GCM time slice integrations. Glob Planet Change 42:83–105

ISMASS Committee (2004) Recommendations for the collection and synthesis of Antarctic Ice Sheet mass balance data. Glob Planet Change 42:1–15

Kaspari S, Mayewski PA, Dixon DA, Spikes VB, Sneed SB, Handley MJ, Hamilton GS (2004) Climate variability in West Antarctica derived from annual accumulation-rate records from ITASE firn/ice cores. Ann Glaciol 39:585–594

Krinner G, Genthon C (1997) The Antarctic surface mass balance in a stretched grid general circulation model. Ann Glaciol 25:73–78

Krinner G, Genthon C (1998) GCM simulations of the last glacial maximum surface climate of Greenland and Antarctica. Clim Dyn 14:741–758

Krinner G, Genthon C (1999) Altitude dependence of the ice sheet surface climate. Geophys Res Lett 26:2227–2230

Krinner G, Werner M (2003) Impact of precipitation seasonality changes on isotopic signals in polar ice cores: a multi-model analysis. Earth Planet Sci Lett 216:525–538

Krinner G, Genthon C, Jouzel J (1997a) GCM analysis of local influences on ice core δ signals. Geophys Res Lett 24:2825–2828

Krinner G, Genthon C, Li ZX, Le Van P (1997b) Studies of the Antarctic climate with a stretched grid GCM. J Geophys Res 102:13731–13745

Krinner G, Mangerud J, Jakobsson M, Crucifix M, Ritz C, Svendsen JI (2004) Enhanced ice sheet growth in Eurasia owing to adjacent ice-dammed lakes. Nature 427:429–432

Kushner PJ, Held IM, Delworth TL (2001) Southern hemisphere atmospheric circulation response to global warming. J Clim 14:2238–2249

Kwok R, Comiso JC (2002) Spatial patterns of variability in Antarctic surface temperature—connections to the southern hemisphere Annular Mode and the Southern Oscillation. Geophys Res Lett 29: 50. DOI 10.1029/2002GL015415

Lachlan-Cope T, Connolley W, Turner J (2001a) The role of non-axisymmetric Antarctic orography in forcing the observed pattern of variability of the Antarctic climate. Geophy Res Lett 28:4111–4114

Lachlan-Cope T, Ladkin R, Turner J, Davison P (2001b) Observations of cloud and precipitation particles on the Avery Plateau, Antarctic Peninsula. Antarct Sci 13:339–348

van Lipzig NPM, van Meijgaard E, Oerlemans J (2002) Temperature sensitivity of the Antarctic Surface Mass Balance in a regional atmospheric climate model. J Clim 15:2758–2774

Listen GE, Winther J-G (2005) Antarctic surface and subsurface snow and ice melt fluxes. J Clim 18:1469–1481

Magand M, Frezzotti M, Pourchet M, Stenni B, Genoni L, Fily M (2004). Climate variability along latitudinal and longitudinal transects in East Antarctica. Ann Glaciol 39:351–358

Marshall GJ, Scott PA, Turner J, Connolley WM, King JC, Lachlan-Cope TA (2004) Causes of exceptional atmospheric circulation changes in the southern hemisphere. Geophys Res Lett 31: L14205. DOI 10.1029/2004GL019952

Marti O, Braconnot P, Bellier J, Benshila R, Bony S, Brockmann P, Cadule P, Caubel A, Denvil S, Dufresne JL, Fairhead L, Filiberti MA, Foujols MA, Fichefet T, Friedlingstein P, Grandpeix JY, Hourdin F, Krinner G, Lévy C, Madec G, Musat I, de Noblet-Ducoudré N, Polcher J, Talandier C (2005). The new IPSL climate system model: IPSL-CM4. Note du Pôle de Modélisation n. 26, IPSL, ISSN 1288–1619. http://www.dods.ipsl.jussieu.fr/omamce/IPSLCM4/Doc-IPSLCM4/

Massom RA, Pook MJ, Comiso JC, Adams N, Turner J, Lachlan-Cope T, Gibson TT (2004) Precipitation over the interior East Antarctic Ice Sheet related to midlatitude blocking-high activity. J Clim 17:1914–1928

Masson-Delmotte V, Kageyama M, Braconnot P, Charbit S, Krinner G, Ritz C, Guilyardi E, Jouzel J, Abe-Ouchi A, Crucifix M, Gladstone RM, Hewitt CD, Kitoh A, Legrande A, Marti O, Merkel U, Motoi T, Ohgaito R, Otto-Bliesner B, Peltier WR, Ross I, Valdez PJ, Vettoretti G, Weber SL, Wolk F (2006) Past and future polar amplification of climate change: climate model intercomparisons and ice-core constraints. Clim Dyn 26:513–529

Mätzler C (1987) Applications of the interaction of microwaves with the natural snow cover. Remote Sens Rev 2:259–387

Miller L, Douglas BC (2004) Mass and volume contributions to twentieth-century global sea level rise. Nature 428:406–409

Minikin A, Wagenbach D, Graf W, Kipfstuhl S (1994) Spatial and temporal variations of the snow chemistry at the central Filchner Ronne Ice Shelf, Antarctica. Ann Glaciol 20:440–447

Monaghan AJ, Bromwich DH, Wang S-H (2006) Recent trends in Antarctic snow accumulation from Polar MM5. Philos Trans R Soc Lond A 364:1683–1708

Mosley-Thompson E, Paskievitch JF, Gow AJ, Thompson LG (1998) Late 20th century increase in South Pole snow accumulation. J Geophys Res 104:3877–3886

Moritz RE, Bitz CM, Steig EJ (2002) Dynamics of recent climate change in the Arctic. Science 297:1497–1502

Murray R, Simmonds I (1991) A numerical scheme for tracking cyclone centres from digital data. Part I development and operation of the scheme. Aust Meteorol Mag 39:167–180

Noone D, Simmonds I (1998) Implications for the interpretation of ice-core isotope data from analysis of modelled Antarctic precipitation. Ann Glaciol 27:398–402

Noone D, Turner J, Mulvaney R (1999) Atmospheric signals and characteristics of accumulation in Dronning Maud Land, Antarctica. J Geophys Res 104:19191–19211

Ohmura A, Wild M, Bengtsson L (1996) A possible change in mass balance of Greenland and Antarctic ice sheets in the coming century. J Clim 9:2124–2135

Parrenin F, Rémy F, Ritz C, Siegert MJ, Jouzel J (2004) New modeling of the Vostok ice flow line and implication for the glaciological chronology of the Vostok ice core. J Geophys Res 109:D20102. DOI 10.1029/2004JD004561

Pfeffer WT, Meier MF, Illangasekare HT (1991) Retention of Greenland runoff by refreezing: implications for projected future sea level change. J Geophys Res 96:22117–22124

Phillpot HR, Zillman JW (1970) The surface temperature inversion over the Antarctic continent. J Geophys Res 75:4161–4169

Pourchet M, Magand O, Frezzotti M, Ekaykin A, Winther JG (2003). Radionuclides deposition over Antarctica. J Environ Radioactivity 68:137–158

Reijmer CH, van den Broeke MR, Schelle MP (2002) Air parcel trajectories and snowfall related to five deep drilling locations in Antarctica based on the ERA-15 dataset. J Clim 15:1957–1968

Robin G (1977) Ice cores and climatic changes. Philos Trans R Soc Lond B 280:143–168

Russell A, McGregor GR, Marshall GJ (2004) An examination of the precipitation delivery mechanisms for Dolleman Island, eastern Antarctic Peninsula. Tellus 56A:501–513

Shindell DT, Schmidt GA (2004) Southern hemisphere climate response to ozone changes and greenhouse gas increases. Geophys Res Lett 31:L18209

Simmonds I (1985) Analysis of the ''Spinup'' of a general circulation model. J Geophys Res 90:5637–5660

Simmonds I (2003) Modes of atmospheric variability over the Southern Ocean. J Geophys Res 108: 8078. DOI 10.1029/2000JC000542

Simmonds I, Keay K (2000) Mean southern hemisphere extratropical cyclone behaviour in the 40-year NCEP-NCAR analysis. J Clim 13:873–885

Simmonds I, Murray RJ (1999) Southern extratropical cyclone behaviour in ECMWF analyses during the FROST Special Observing Periods. Weather Forecast 14:878–891

Simmonds I, Wu X (1993) Cyclone behaviour response to changes in winter southern hemisphere sea-ice concentration. Q J R Meteorol Soc 119:1121–1148

Smith BT, Van Ommen TD, Morgan VI (2002) Distribution of oxygen isotope ratios and snow accumulation rates in Wilhelm II Land, East Antarctica. Ann Glaciol 35:107–110

Stone DA, Weaver AJ, Stouffer RJ (2001) Projection of climate change onto modes of atmospheric variability. J Clim 14:3551–3565

Taylor KC, White JWC, Severinghaus JP, Brook EJ, Mayewski PA, Alley RB, Steig EJ, Spencer MK, Meyerson E, Meese DA, Lamorey GW, Grachev A, Gow AJ, Barnett BA (2004) Abrupt climate change around 22 ka on the Siple Coast of Antarctica. Q Sci Rev 23:7–15

Thomas R, Rignot E, Casassa G, Kanagaratnam P, Acuña C, Akins T, Brecher H, Frederick E, Gogineni P, Krabill W, Manizade S, Ramamoorthy H, Rivera A, Russell R, Sonntag J, Swift R, Yungel J, Zwally J (2004) Accelerated sea-level rise from West Antarctica. Science 306:255–258

Thompson DWJ, Solomon S (2002) Interpretation of recent southern hemisphere climate change. Science 296:895–899

Thompson SL, Pollard D (1997) Greenland and Antarctic mass balances for present and doubled atmospheric CO_2 from the GENESIS Version-2 Global Climate Model. J Clim 10:871–900

Torinesi O, Fily M, Genthon C (2003) Variability and trends of the summer melt period of Antarctic ice margins since 1980 from microwave sensors. J Clim 16:1047–1060

Turner J, Lachlan-Cope TA, Thomas JP, Colwell S (1995) The synoptic origins of precipitation over the Antarctic Peninsula. Antarct Sci 7:327–337

Turner J, Harangozo SA, Marshall GJ, King JC, Colwell SR (2002) Anomalous atmospheric circulation over the Weddell Sea, Antarctica during the austral summer of 2001/2 resulting in extreme sea ice conditions. Geophys Res Lett 29:2160. DOI 10.1029/2002GL015565

Turner J, Lachlan-Cope TA, Colwell S, Marshall GJ, Connolley WM (2006) Significant warming of the Antarctic winter troposphere. Science 311:1914–1917

van de Berg WJ, van den Broeke MR, Reijmer CH (2006) Reassessment of the Antarctic surface mass balance using calibrated input of a regional atmospheric climate model. J Geophys Res 111:D11104. DOI: 10.1029/2005JD006495

van den Broeke MR (1997) Spatial and temporal variation of sublimation on Antarctica: results of a high-resolution general circulation model. J Geophys Res 102:29765–29777

van den Broeke MR (2005) Strong surface melting preceded collapse of Antarctic peninsula ice shelf. Geophys Res Lett 32:L12815

van den Broeke MR, van der Berg WJ, van Meijgaard E (2006) Snowfall in coastal West Antarctica much greater than previously assumed. Geophys Res Lett 33:L02505

Vaughan DG, Bamber JL, Giovinetto M, Russell J, Cooper APR (1999) Reassessment of net surface mass balance in Antarctica. J Clim 12:933–946

Vaughan DG, Marshall GJ, Connolley WM, Parkinson C, Mulvaney R, Hogson DA, King JC, Pudsey CJ, Turner J (2003) Recent rapid regional climate warming on the Antarctic Peninsula. Clim Change 60:243–274

Watanabe O, Jouzel J, Johnsen S, Parrenin P, Shoji H, Yoshida N (2003) Homogeneous climate variability across East Antarctica over the past three cycles. Nature 422:509–512

Watkins AB, Simmonds I (1995) Sensitivity of numerical prognoses to Antarctic sea ice distribution. J Geophys Res 100:22681–22696

Wild M, Calanca P, Scherrer S, Ohmura A (2003) Effects of polar ice sheets on global sea level in high-resolution greenhouse scenarios. J Geophys Res 108:4165

Yamazaki K (1994) Moisture budget in the Antarctic atmosphere. In: Jones HG, Davies TD, Ohmura A, Morris EM (eds) Snow and ice covers: interactions with the atmosphere and ecosystems. IAHS Publication No. 233, IAHS Press, pp 61–67

Zwally HJ, Abdalati W, Herring T, Larson K, Saba J, Steffen K (2002) Surface melt-induced acceleration of Greenland Ice-Sheet flow. Science 297:218–222